Saturated Vectorial Control of Multi-phase Synchronous Motors

R. Zanasi *, **M. Fei** *

* *Information Engineering Department, University of Modena and Reggio Emilia, Via Vignolese 905, 41100 Modena, Italy (e-mail: roberto.zanasi@unimore.it, marco.fei@unimore.it)*

Abstract. This paper deals with the torque control of multi-phase permanent magnet synchronous machines. The dynamic model of these motors is obtained using the Power-Oriented Graphs technique. This graphical modeling technique allows to write the dynamic equations of the system in a very compact form. Starting from the dynamic equations, a torque control law with saturated input voltages is proposed based on a new current vector approach for describing the voltage constraint. Some simulation results validate the proposed control law.

1. INTRODUCTION

In this paper is proposed a vectorial torque control with saturated input voltages of multi-phase synchronous motors. The proposed control is the generalization of the current vectorial control given in Zanasi and Grossi [2009]. The classical dynamic model of multi-phase synchronous motors with an odd number of phases can be found in Vas [1990] - Kestelyn et al. [2004]. The model is obtained using a Lagrangian approach in the frame of the Power-Oriented Graphs (POG) technique, see Zanasi [1994]-Zanasi and Grossi [2008]. In the present paper all the first m_s Fourier series coefficients of the rotor flux are considered and the proposed control law operates in a full m_s-dimensional subspace. The paper is organized as follows. In Sec. 2 the POG dynamic model of the multi-phase synchronous motors is described. In Sec. 3 and 4 the new vectorial torque control is presented. Finally, in Sec. 5 some simulation results are reported.

1.1 Notations

Row matrices are denoted as: $[\![\, R_i \,]\!]_{1:n}^{i} = [\, R_1 \;\; R_2 \;\; \dots \;\; R_n \,]$. Column and diagonal matrices are denoted as:

$$[\![\, R_i \,]\!]_{1:n}^{i} = \begin{bmatrix} R_1 \\ R_2 \\ \vdots \\ R_n \end{bmatrix}, \qquad [\![\, R_i \,]\!]_{1:n}^{i} = \begin{bmatrix} R_1 & & & \\ & R_2 & & \\ & & \ddots & \\ & & & R_n \end{bmatrix}$$

and full matrices as:

$$[\![\, R_{i,j} \,]\!]_{1:n\;1:m}^{i\;\;j} = \begin{bmatrix} R_{11} & R_{12} & \cdots & R_{1m} \\ R_{21} & R_{22} & \cdots & R_{2m} \\ \vdots & \vdots & \ddots & \vdots \\ R_{n1} & R_{n2} & \cdots & R_{nm} \end{bmatrix}.$$

The symbol "$\sum_{n=a:d}^{b} c_n = c_a + c_{a+d} + c_{a+2d} + \dots$" will be used to represent the sum of a succession of numbers c_n where the index n ranges from a to b with increment d, that is, using the Matlab symbology, $n = [a : d : b]$.

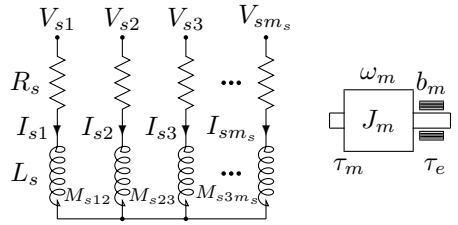

Figure 1. Basic structure of a multi-phase synchronous motor.

m_s	number of motor phases;
p	number of polar expansions;
θ, θ_m	electric and rotor angular positions: $\theta = p\,\theta_m$;
ω, ω_m	electric and rotor angular velocities: $\omega = p\,\omega_m$;
R_s	i-th stator phase resistance;
L_s	i-th stator phase self induction coefficient;
M_{s0}	maximum mutual inductance between phases;
$\phi_c(\theta)$	total rotor flux chained with stator phase 1;
φ_c	maximum value of function $\phi_c(\theta)$;
J_m	rotor moment of inertia;
b_m	rotor linear friction coefficient;
τ_m	electromotive torque acting on the rotor;
τ_e	external load torque acting on the rotor;
γ_s	basic angular displacement ($\gamma_s = 2\pi/m_s$)

Table 1. Parameters of the synchronous motor.

2. ELECTRICAL MOTORS MODELLING

The basic structure of a permanent magnet synchronous motor with an *odd* number m_s of star-connected phases is shown in Fig. 1 and its parameters are shown in Tab. 1.

Let us introduce the following current and voltage stator vectors:

$${}^{t}\mathbf{I}_s = [I_{s1}\; I_{s2}\; \cdots\; I_{sm_s}]^{\mathrm{T}}, \quad {}^{t}\mathbf{V}_s = [V_{s1}\; V_{s2}\; \cdots\; V_{sm_s}]^{\mathrm{T}}. \quad (1)$$

Using a "POG-Lagrangian" approach, see Zanasi and Grossi [2008] Zanasi and Grossi [2009], and the following transformation matrix:

$${}^{\omega}\mathbf{T}_t = \sqrt{\frac{2}{m_s}} \left[\!\!\left[\begin{matrix} \cos(k\,(\theta - h\,\gamma_s)) \\ \sin(k\,(\theta - h\,\gamma_s)) \end{matrix} \right]\!\!\right]_{1:2:m_s-2\;\;0:m_s-1}^{k\qquad\quad h} \quad (2)$$

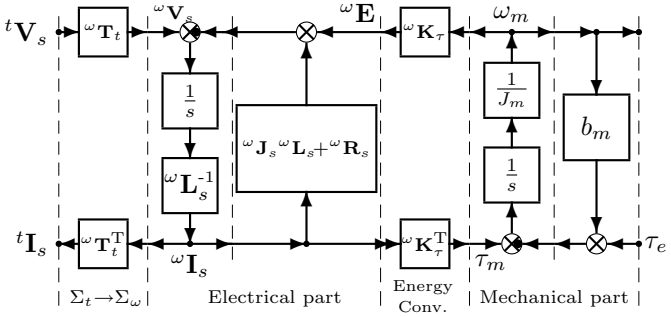

Figure 2. POG scheme of the electrical motor in frame Σ_ω.

one obtains the following transformed and reduced system:

$$\left[\begin{array}{c|c} {}^{\omega}\mathbf{L}_s & 0 \\ \hline 0 & J_m \end{array}\right]\left[\begin{array}{c} {}^{\omega}\dot{\mathbf{I}}_s \\ \hline \dot{\omega}_m \end{array}\right]=-\left[\begin{array}{c|c} {}^{\omega}\mathbf{R}_s+{}^{\omega}\mathbf{L}_s\,{}^{\omega}\mathbf{J}_s & {}^{\omega}\mathbf{K}_\tau(\theta) \\ \hline -{}^{\omega}\mathbf{K}_\tau^{\mathrm{T}}(\theta) & b_m \end{array}\right]\left[\begin{array}{c} {}^{\omega}\mathbf{I}_s \\ \hline \omega_m \end{array}\right]+\left[\begin{array}{c} {}^{\omega}\mathbf{V}_s \\ \hline -\tau_e \end{array}\right] \quad (3)$$

where matrices ${}^{\omega}\mathbf{L}_s$, ${}^{\omega}\mathbf{J}_s$ and ${}^{\omega}\mathbf{R}_s$ are defined as follows:

$${}^{\omega}\mathbf{L}_s=\begin{bmatrix} L_{se} & 0 & 0 & \cdots & 0 \\ 0 & L_{se} & 0 & \cdots & 0 \\ 0 & 0 & L_{s0} & \cdots & 0 \\ \vdots & \vdots & \vdots & \ddots & \vdots \\ 0 & 0 & 0 & \cdots & L_{s0} \end{bmatrix}, \quad {}^{\omega}\mathbf{J}_s=\Big\|\begin{bmatrix} 0 & -k\,\omega \\ k\,\omega & 0 \end{bmatrix}\Big\|_{1:2:m_s-2}^{k}$$

$${}^{\omega}\mathbf{R}_s=\Big[\!\!\Big[\, R_s \,\Big]\!\!\Big]_{1:m_s-1}^{i}$$

$L_{se}=L_{s0}+\frac{m_s}{2}M_{s0}$ and $L_{s0}=L_s-M_{s0}$. Vectors ${}^{\omega}\mathbf{I}_s={}^{t}\mathbf{T}_{\omega}^{\mathrm{T}}\,{}^{t}\mathbf{I}_s$, ${}^{\omega}\mathbf{V}_s={}^{t}\mathbf{T}_{\omega}^{\mathrm{T}}\,{}^{t}\mathbf{V}_s$ are defined as:

$${}^{\omega}\mathbf{I}_s=\Big\|\begin{bmatrix} {}^{\omega}\mathbf{I}_{sk} \end{bmatrix}\Big\|_{1:2:m_s-2}^{k}=\Big\|\begin{bmatrix} I_{dk} \\ I_{qk} \end{bmatrix}\Big\|_{1:2:m_s-2}^{k}, \quad {}^{\omega}\mathbf{V}_s=\Big\|\begin{bmatrix} {}^{\omega}\mathbf{V}_{sk} \end{bmatrix}\Big\|_{1:2:m_s-2}^{k}=\Big\|\begin{bmatrix} V_{dk} \\ V_{qk} \end{bmatrix}\Big\|_{1:2:m_s-2}^{k}$$

where I_{dk}, I_{qk}, V_{dk} and V_{qk} are, respectively, the *direct* and *quadrature* components of the current and voltage vectors ${}^{\omega}\mathbf{I}_s$ and ${}^{\omega}\mathbf{V}_s$. Note that using transformation ${}^{\omega}\mathbf{V}_s={}^{t}\mathbf{T}_{\omega}^{\mathrm{T}}\,{}^{t}\mathbf{V}_s$ the original state space Σ_t has been transformed into $(m_s-1)/2$ two-dimensional orthogonal subspaces named $\Sigma_{\omega k}$ with $k\in\{1:2:m_s-2\}$. It can be shown, see Zanasi and Grossi [2008], that when the rotor flux function $\bar{\phi}(\theta)$ has the structure $\bar{\phi}(\theta)=\sum_{i=1:2}^{m_s-2}a_i\cos(i\,\theta)$, the torque vector ${}^{\omega}\mathbf{K}_\tau(\theta)$ is constant:

$${}^{\omega}\mathbf{K}_\tau=\varphi_c\,p\,\sqrt{\frac{m_s}{2}}\Big\|\begin{bmatrix} 0 \\ k\,a_k \end{bmatrix}\Big\|_{1:2:m_s-2}^{k}=\Big\|\begin{bmatrix} {}^{\omega}\mathbf{K}_{\tau k} \end{bmatrix}\Big\|_{1:2:m_s-2}^{k}=\Big\|\begin{bmatrix} K_{dk} \\ K_{qk} \end{bmatrix}\Big\|_{1:2:m_s-2}^{k} \quad (4)$$

The POG block scheme of the synchronous motor in the transformed space Σ_ω, see eq. (3), is shown in Fig. 2. The Power-Oriented Graphs is an energy-based technique suitable for modeling physical systems, see Zanasi [1991]-Zanasi [1994].

2.1 Balanced voltages

Let us now consider the case of a voltage stator vector ${}^{t}\mathbf{V}_s$ obtained as the sum of $(m_s-1)/2$ balanced input voltage vectors at different frequency:

$${}^{t}\mathbf{V}_s=\Big[\!\!\Big[\, V_{sh} \,\Big]\!\!\Big]_{1:m_s}^{h}=\sum_{j=1:2}^{m_s-2}\Big[\!\!\Big[V_{mj}\,\cos(j((h-1)\gamma_s-\theta-\theta_{sj})) \Big]\!\!\Big]_{1:m_s}^{h} \quad (5)$$

where V_{mj} is the amplitude of the input voltage component at frequency j and θ_{sj} is a proper initial phase shift. The amplitudes of components V_{sh} of vector ${}^{t}\mathbf{V}_s$ are bounded by the maximum value V_{max}:

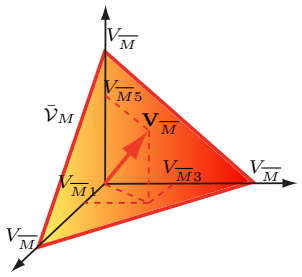

Figure 3. Graphical representation of convex set $\bar{\mathcal{V}}_M$ for $m_s=7$.

$$|V_{sh}|\le\sum_{j=1:2}^{m_s-2}V_{mj}\le V_{max}, \quad (6)$$

for $h=\{1,2,\ldots m_s\}$. The transformed vector ${}^{\omega}\mathbf{V}_s={}^{t}\mathbf{T}_{\omega}^{\mathrm{T}}\,{}^{t}\mathbf{V}_s\in\mathbb{R}^{m_s-1}$ has the following structure:

$${}^{\omega}\mathbf{V}_s=\sqrt{\frac{m_s}{2}}\Big\|\begin{bmatrix} V_{mk}\,\cos(k\,\theta_{sk}) \\ V_{mk}\,\sin(k\,\theta_{sk}) \end{bmatrix}\Big\|_{1:2:m_s-2}^{k}. \quad (7)$$

Using the following bijective correspondence between two-dimensional vectors and complex numbers:

$$\begin{bmatrix}\cos(k\,\theta_{sk})\\ \sin(k\,\theta_{sk})\end{bmatrix} \quad\leftrightarrow\quad \cos(k\,\theta_{sk})+j\,\sin(k\,\theta_{sk})=e^{j\,k\,\theta_{sk}}$$

the expression (7) can be rewritten in the equivalent way:

$${}^{\omega}\overline{\mathbf{V}}_s=\sqrt{\frac{m_s}{2}}\Big\|\begin{bmatrix} V_{mk}\,e^{j\,k\,\theta_{sk}} \end{bmatrix}\Big\|_{1:2:m_s-2}^{k}=\Big\|\begin{bmatrix} \overline{V}_{sk} \end{bmatrix}\Big\|_{1:2:m_s-2}^{k} \quad (8)$$

where ${}^{\omega}\overline{\mathbf{V}}_s\in\mathbb{C}^{\frac{m_s-1}{2}}$ is a vector of complex numbers. Expression (8) shows that all the balanced input voltage vectors at frequency k with amplitude $V_{mk}=V_{mj}$, see (5), are transformed into vectors $\overline{V}_{sk}$ with modulus $V_{Mk}=\sqrt{\frac{m_s}{2}}\,V_{mk}$ in the two-dimensional subspace $\Sigma_{\omega k}$. Defined the vector $\mathbf{V}_M\in\mathbb{R}^{\frac{m_s-1}{2}}$ as:

$$\mathbf{V}_M=\Big\|\begin{bmatrix} V_{Mk} \end{bmatrix}\Big\|_{1:2:m_s-2}^{k}=\Big\|\begin{bmatrix} |\overline{V}_{sk}| \end{bmatrix}\Big\|_{1:2:m_s-2}^{k}=\Big\|\begin{bmatrix} \sqrt{\frac{m_s}{2}}\,V_{mk} \end{bmatrix}\Big\|_{1:2:m_s-2}^{k},$$

the voltage constraint (6), multiplied by constant $\sqrt{\frac{m_s}{2}}$, becomes the following 1-norm constraint on vector $\mathbf{V}_M$:

$$\|\,\mathbf{V}_M\,\|_1=\sum_{k=1:2}^{m_s-2}V_{Mk}\le\sqrt{\frac{m_s}{2}}\,V_{max}=V_{\overline{M}}. \quad (9)$$

The set of all the vectors $\mathbf{V}_{\overline{M}}$ that satisfy the equation:

$$\|\,\mathbf{V}_{\overline{M}}\,\|_1=\sum_{k=1:2}^{m_s-2}V_{\overline{M}k}=V_{\overline{M}} \quad (10)$$

is a convex set $\bar{\mathcal{V}}_M$ with dimension $\frac{m_s-1}{2}-1$ that represents the maximum of the voltage constraint (6) in frame Σ_ω. When $m_s=7$ the set $\bar{\mathcal{V}}_M\in\mathbb{R}^3$ belongs to a plane, see Fig. 3. Each vector $\mathbf{V}_{\overline{M}}\in\bar{\mathcal{V}}_M$ can be written as a convex combination of the standard basis vectors $\mathbf{e}_i$ of subspace $\mathbb{R}^{\frac{m_s-1}{2}}$:

$$\mathbf{V}_{\overline{M}}=V_{\overline{M}}\sum_{i=1}^{\frac{m_s-1}{2}}\beta_i\,\mathbf{e}_i, \qquad 0\le\beta_i\le 1, \quad \sum_{i=1}^{\frac{m_s-1}{2}}\beta_i=1. \quad (11)$$

3. VECTORIAL CONTROL

Let ${}^{\omega}\mathbf{I}_d$ denote the desired phase current vector in frame Σ_ω. When ${}^{\omega}\mathbf{I}_d$ is constant, the condition ${}^{\omega}\mathbf{I}_s = {}^{\omega}\mathbf{I}_d$ can be achieved using the following control:

$$ {}^{\omega}\mathbf{V}_s = ({}^{\omega}\mathbf{R}_s + {}^{\omega}\mathbf{J}_s\,{}^{\omega}\mathbf{L}_s)\,{}^{\omega}\mathbf{I}_s + {}^{\omega}\mathbf{K}_\tau\,\omega_m - \mathbf{K}_c({}^{\omega}\mathbf{I}_s - {}^{\omega}\mathbf{I}_d) \quad (12) $$

where $\mathbf{K}_c > 0$ is a diagonal matrix used for the control design. In steady-state condition when ${}^{\omega}\mathbf{I}_s = {}^{\omega}\mathbf{I}_d$, the control law (12) is equivalent to $(m_s - 1)/2$ two-dimensional decoupled control laws:

$$ {}^{\omega}\mathbf{V}_{sk} = ({}^{\omega}\mathbf{R}_{sk} + {}^{\omega}\mathbf{J}_{sk}\,{}^{\omega}\mathbf{L}_{sk})\,{}^{\omega}\mathbf{I}_{sk} + {}^{\omega}\mathbf{K}_{\tau k}\,\omega_m \quad (13) $$

where:

$$ {}^{\omega}\mathbf{R}_{sk} = \begin{bmatrix} R_s & 0 \\ 0 & R_s \end{bmatrix}, \quad {}^{\omega}\mathbf{J}_{sk}\,{}^{\omega}\mathbf{L}_{sk} = \begin{bmatrix} 0 & -k\,p\,\omega_m L_{sk} \\ k\,p\,\omega_m L_{sk} & 0 \end{bmatrix} $$

and

$$ L_{sk} = \begin{cases} L_{se} & \text{for } k = 1 \\ L_{s0} & \text{for } k \in \{3,\,5,\,7,\ldots,m_s\} \end{cases} $$

each one acting on subspace $\Sigma_{\omega k}$, for $k \in \{1 : 2 : m_s - 2\}$. Using the following bijective correspondences between two-dimensional vectors and complex numbers:

$$ {}^{\omega}\mathbf{I}_{sk} \leftrightarrow \overline{I}_{sk} = I_{dk} + j\,I_{qk}, \quad {}^{\omega}\mathbf{V}_{sk} \leftrightarrow \overline{V}_{sk} = V_{dk} + j\,V_{qk}, $$
$$ {}^{\omega}\mathbf{K}_{\tau k} \leftrightarrow \overline{K}_{\tau k} = K_{dk} + j\,K_{qk}, \quad {}^{\omega}\mathbf{J}_{sk}\,{}^{\omega}\mathbf{L}_{sk} \leftrightarrow j\,k\,p\,\omega_m L_{sk} $$

and ${}^{\omega}\mathbf{R}_{sk} \leftrightarrow R_s$, eq. (13) can be rewritten as follows:

$$ \overline{V}_{sk} = (R_s + j\,k\,p\,\omega_m L_{sk})\overline{I}_{sk} + \overline{K}_{\tau k}\,\omega_m \quad (14) $$

where j is the imaginary unit number. When $\overline{K}_{\tau k} = j\,K_{qk}$ and rewriting relation (14) as follows:

$$ \begin{aligned} \overline{I}_{sk} &= \frac{\overline{V}_{sk} - j\,K_{qk}\,\omega_m}{R_s + j\,k\,p\,\omega_m\,L_{sk}} \\ &= \underbrace{\frac{\overline{V}_{sk}}{R_s + j\,k\,p\,\omega_m\,L_{sk}}}_{\overline{R}_{0k}\,(\omega_m)} + \underbrace{\frac{-j\,K_{qk}\,\omega_m}{R_s + j\,k\,p\,\omega_m\,L_{sk}}}_{\overline{C}_{0k}\,(\omega_m)} \end{aligned} \quad (15) $$

one obtains the "current" control approach proposed in Zanasi and Grossi [2009]. When vector $\overline{V}_{sk}$ varies along the maximum voltage circle having radius $V_{\overline{M}k}$, see eq. 10, relation (15) provides the maximum current circle $\mathcal{C}_k$ corresponding to the limit values for the current vector $\overline{I}_{sk}$, see Fig. 4. The terms $\overline{C}_{0k}\,(\omega_m)$ and $\overline{R}_{0k}\,(\omega_m)$ in (15) represent the center and the radius of the maximum current circle $\mathcal{C}_k$ as a function of the parameter ω_m. When velocity ω_m increases the radius $\overline{R}_{0k}$ of circle $\mathcal{C}_k$ decreases and its center $\overline{C}_{0k}$ moves in the complex plane $\Sigma_{\omega k}$ on a circle with center in $\left(\frac{-K_{qk}}{2\,k\,p\,L_{sk}},\,0\right)$ and radius $\frac{K_{qk}}{2\,k\,p\,L_{sk}}$. A graphical representation of the current circle $\mathcal{C}_k$ on the complex plane $\Sigma_{\omega k}$ for a particular value of ω_m is showed in red in Fig. 4. The projection of circle $\mathcal{C}_k$ on the I_{qk} axis gives the range of all the currents I_{qk} satisfying the voltage constraint $V_{\overline{M}k}$ which can generate torque. Three different operative zones are clearly defined: 1) the interval $[I_{qk\underline{N}},\ I_{qkN}]$ represents the zone in which the torque can be provided using only the quadrature component I_{qk} of the current vector $\overline{I}_{sk}$; 2) the intervals $[I_{qk\underline{M}},\ I_{qk\underline{N}}]$ and $[I_{qkN},\ I_{qkM}]$ represent the zone in which the desired torque can be provided only using a full "d-q" complex vector $\overline{I}_{sk}$; 3) the zone where $I_{qk} > I_{qkM}$ and $I_{qk} < I_{qk\underline{M}}$ is not allowed because it does not satisfy the constraint on the maximum input voltage. coordinates of the projection points shown in Fig. 4 are the following:

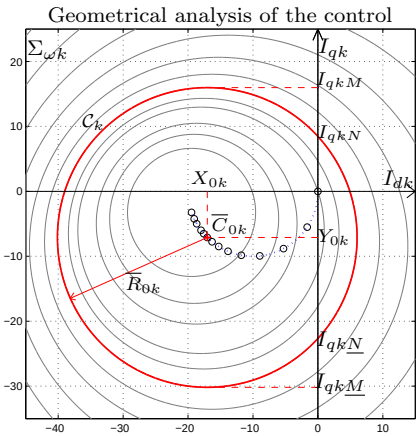

Figure 4. Maximum current circle $\mathcal{C}_k$ in subspace $\Sigma_{\omega k}$.

$$ I_{qkM}(\omega_m) = Y_{0k}(\omega_m) + R_{0k}(\omega_m) \quad (16) $$

$$ I_{qkN}(\omega_m) = Y_{0k}(\omega_m) + \sqrt{R_{0k}^2(\omega_m) - X_{0k}^2(\omega_m)} \quad (17) $$

$$ I_{qk\underline{N}}(\omega_m) = Y_{0k}(\omega_m) - \sqrt{R_{0k}^2(\omega_m) - X_{0k}^2(\omega_m)} \quad (18) $$

$$ I_{qk\underline{M}}(\omega_m) = Y_{0k}(\omega_m) - R_{0k}(\omega_m) \quad (19) $$

where:

$$ R_{0k}(\omega_m) = \left|\overline{R}_{0k}\,(\omega_m)\right|_{|\overline{V}_{sk}| = V_{\overline{M}k}} = \frac{V_{\overline{M}k}}{\sqrt{R_s^2 + k^2\,p^2\,\omega_m^2 L_{sk}^2}}, $$

$$ X_{0k}(\omega_m) = Re(\overline{C}_{0k}\,(\omega_m)) = \frac{-K_{qk}\,k\,p\,\omega_m^2 L_{sk}}{R_s^2 + k^2\,p^2\,\omega_m^2 L_{sk}^2}, $$

$$ Y_{0k}(\omega_m) = Im(\overline{C}_{0k}\,(\omega_m)) = \frac{-K_{qk}\,\omega_m R_s}{R_s^2 + k^2\,p^2\,\omega_m^2 L_{sk}^2}. $$

Using the projection points I_{qkN} and $I_{qk\underline{N}}$ one can define the following current vectors:

$$ {}^{\omega}\mathbf{I}_{qN} = \left\| \begin{bmatrix} 0 \\ I_{qkN}(\omega_m) \end{bmatrix} \right\|_{1:2:m_s-2}^{k}, \quad {}^{\omega}\mathbf{I}_{q\underline{N}} = \left\| \begin{bmatrix} 0 \\ I_{qk\underline{N}}(\omega_m) \end{bmatrix} \right\|_{1:2:m_s-2}^{k}. \quad (20) $$

On the basis of the maximum and minimum points $\overline{I}_{kM} = X_{0k} + j\,I_{qkM}$ and $\overline{I}_{km} = X_{0k} + j\,I_{qk\underline{M}}$ shown in Fig. 4 one can define the following current vectors:

$$ {}^{\omega}\mathbf{I}_{M} = \left\| \begin{bmatrix} X_{0k}(\omega_m) \\ I_{qkM}(\omega_m) \end{bmatrix} \right\|_{1:2:m_s-2}^{k}, \quad {}^{\omega}\mathbf{I}_{\underline{M}} = \left\| \begin{bmatrix} X_{0k}(\omega_m) \\ I_{qk\underline{M}}(\omega_m) \end{bmatrix} \right\|_{1:2:m_s-2}^{k}. \quad (21) $$

4. TORQUE CONTROL

The torque τ_d generated by the desired current vector ${}^{\omega}\mathbf{I}_d$ is given by relation:

$$ \tau_d = {}^{\omega}\mathbf{K}_\tau^{\mathrm{T}}\,{}^{\omega}\mathbf{I}_d. \quad (22) $$

Torque τ_d can be controlled by choosing a current vector ${}^{\omega}\mathbf{I}_d$ not exceeding the constraint on the maximum input voltage V_{max} and minimizing the internal power dissipations. Depending on the working conditions, the following three different control strategies can be used.

4.1 Torque control with minimum dissipation

The current vector ${}^{\omega}\mathbf{I}_{md}$ which satisfies relation (22) and minimizes the power dissipation is the vector with the minimum modulus parallel to vector ${}^{\omega}\mathbf{K}_\tau$:

$$ {}^{\omega}\mathbf{I}_{md} = \frac{\tau_d}{|{}^{\omega}\mathbf{K}_\tau|}\,{}^{\omega}\hat{\mathbf{K}}_\tau = \frac{{}^{\omega}\mathbf{K}_\tau}{|{}^{\omega}\mathbf{K}_\tau|^2}\,\tau_d \tag{23} $$

where ${}^{\omega}\hat{\mathbf{K}}_\tau$ denotes the versor of vector ${}^{\omega}\mathbf{K}_\tau$. When vector ${}^{\omega}\mathbf{K}_\tau$ is costant, see (4), the expression (23) can be written as:

$$ {}^{\omega}\mathbf{I}_{md} = \left\| \begin{bmatrix} 0 \\ \tau_d\,\widetilde{K}_k \end{bmatrix} \right\|_{1:2:m_s-2}^{k} \quad \text{where} \quad \widetilde{K}_k = \frac{K_{qk}}{|{}^{\omega}\mathbf{K}_\tau|^2}. \tag{24} $$

Substituting equation (24) in (13) and using the voltage constraint (10) one obtains the following equation:

$$ \sum_{k=1:2}^{m_s-2} \underbrace{\sqrt{(L_{sk}\,k p\omega_m \tau_d \widetilde{K}_k)^2 + (R_s \tau_d \widetilde{K}_k + K_{qk}\omega_m)^2}}_{V_{\overline{M}k}} = V_{\overline{M}}. \tag{25} $$

Given ω_m, equation (25) can be numerically solved with respect to τ_d in order to obtain the maximum and minimum torques $\tau_N(\omega_m)$ and $\tau_{\underline{N}}(\omega_m)$ satisfying minimum dissipation and the voltage constraint. Using equation (24), the current vectors ${}^{\omega}\mathbf{I}_N$ and ${}^{\omega}\mathbf{I}_{\underline{N}}$ corresponding to the maximum and minimum torques $\tau_N(\omega_m)$ and $\tau_{\underline{N}}(\omega_m)$ are the current vector associated to vectors (20):

$$ {}^{\omega}\mathbf{I}_N = \left\| \begin{bmatrix} 0 \\ \tau_N\,\widetilde{K}_k \end{bmatrix} \right\|_{1:2:m_s-2}^{k} = {}^{\omega}\mathbf{I}_{qN}, \qquad {}^{\omega}\mathbf{I}_{\underline{N}} = \left\| \begin{bmatrix} 0 \\ \tau_{\underline{N}}\,\widetilde{K}_k \end{bmatrix} \right\|_{1:2:m_s-2}^{k} = {}^{\omega}\mathbf{I}_{q\underline{N}}. $$

The desired torque τ_d can be obtained with minimum current vector ${}^{\omega}\mathbf{I}_{md}$ only if ${}^{\omega}\mathbf{I}_{\underline{N}} \le {}^{\omega}\mathbf{I}_{md} \le {}^{\omega}\mathbf{I}_N$ or, in equivalent way, if $\tau_{\underline{N}}(\omega_m) \le \tau_d < \tau_N(\omega_m)$. In Fig. 6 the two curves $\tau_N(\omega_m)$ and $\tau_{\underline{N}}(\omega_m)$ define in the torque plane the green zone that represents the region where the desired torque τ_d it can be provided minimizing the power dissipation. Due to the symmetric structure of the considered electric motor, it can be easily shown that $\tau_{\underline{N}}(\omega_m) = -\tau_N(-\omega_m)$.
From (25) it can be numerically obtained the velocity ω_L that represents the motor velocity ω_m where $\tau_{\underline{N}}(\omega_m) = \tau_N(\omega_m)$. When $\omega_m > \omega_L$ this control can not be used because the voltage constraint is not respected.

4.2 Maximum torque control

From Fig. 4 is clear that the maximum and minimum torques $\tau_M(\omega_m)$ and $\tau_{\underline{M}}(\omega_m)$ can be obtained as follows:

$$ \tau_M(\omega_m) = {}^{\omega}\mathbf{K}_\tau^{\mathrm{T}}\,{}^{\omega}\mathbf{I}_M, \qquad \tau_{\underline{M}}(\omega_m) = {}^{\omega}\mathbf{K}_\tau^{\mathrm{T}}\,{}^{\omega}\mathbf{I}_{\underline{M}}. \tag{26} $$

Substituting (4) and (21) in (26) one obtains the relations:

$$ \begin{aligned} \tau_M(\omega_m) &= \sum_{k=1:2}^{m_s-2} K_{qk}\,Y_{0k}(\omega_m) + \sum_{k=1:2}^{m_s-2} K_{qk}\,R_{0k}(\omega_m) \\ &= \tau_0(\omega_m) + \mathbf{K}_b^{\mathrm{T}}\,\mathbf{V}_{\overline{M}} \\ \tau_{\underline{M}}(\omega_m) &= \tau_0(\omega_m) - \mathbf{K}_b^{\mathrm{T}}\,\mathbf{V}_{\overline{M}} \end{aligned} \tag{27} $$

where torque $\tau_0(\omega_m)$ and vector $\mathbf{K}_b$ are defined as follows:

$$ \tau_0(\omega_m) = -\frac{m_s}{2}\,\varphi_c^2 \sum_{k=1:2}^{m_s-2} \frac{k^2\,p^2\,a_k^2\,\omega_m R_s}{R_s^2 + k^2\,p^2\,\omega_m^2 L_{sk}^2} $$

$$ \mathbf{K}_b = \left\| \begin{bmatrix} K_{bk} \end{bmatrix} \right\|_{1:2:m_s-2}^{k} = \varphi_c \sqrt{\frac{m_s}{2}} \left\| \begin{bmatrix} \dfrac{p\,k\,a_k}{\sqrt{R_s^2 + k^2\,p^2\,\omega_m^2\,L_{sk}^2}} \end{bmatrix} \right\|_{1:2:m_s-2}^{k}. $$

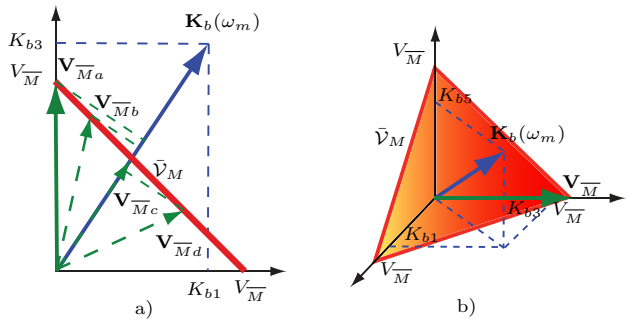

Figure 5. Vectors $\mathbf{V}_{\overline{M}}$ and $\mathbf{K}_b$: a) for $m_s = 5$; b) for $m_s = 7$.

From (27) it is evident that both the maximum and minimum torques τ_M and $\tau_{\underline{M}}$ can be obtained maximizing the scalar product $\mathbf{K}_b^{\mathrm{T}}\,\mathbf{V}_{\overline{M}}$. Since $\mathbf{V}_{\overline{M}} \in \bar{\mathcal{V}}_M$, see Fig. 5, the product $\mathbf{K}_b^{\mathrm{T}}\,\mathbf{V}_{\overline{M}}$ is maximum when the components $V_{\overline{M}k}$ of vector $\mathbf{V}_{\overline{M}}$ are chosen as:

$$ V_{\overline{M}k} = \begin{cases} V_{\overline{M}} & \text{if } |K_{bk}| = \max\{|K_{bi}|,\ i \in [1:2:m_s-2]\} \\ 0 & \text{otherwise} \end{cases} \tag{28} $$

The case of $m_s = 5$ is represented in Fig. 5.a where $\mathbf{V}_{\overline{M}a}$, $\mathbf{V}_{\overline{M}b}$, $\mathbf{V}_{\overline{M}c}$, $\mathbf{V}_{\overline{M}d} \in \bar{\mathcal{V}}_M$ and $\mathbf{K}_b$ is a vector moving in subspace $\mathbb{R}^2$. The vectors $\mathbf{V}_{\overline{M}b}$, $\mathbf{V}_{\overline{M}c}$ and $\mathbf{V}_{\overline{M}d}$ do not maximize the scalar product because their projections onto $\mathbf{K}_b$ are smaller than the projection of vector $\mathbf{V}_{\overline{M}a}$. In this case $\mathbf{V}_{\overline{M}} = \mathbf{V}_{\overline{M}a}$ is the vector that maximizes the scalar product $\mathbf{K}_b^{\mathrm{T}}\,\mathbf{V}_{\overline{M}}$. In the general case the product $\mathbf{K}_b^{\mathrm{T}}\,\mathbf{V}_{\overline{M}}$ is maximum, see eq. (28), when the maximum value $V_{\overline{M}}$ is given only to the component $V_{\overline{M}k}$ corresponding to the component K_{bk} of vector $\mathbf{K}_b$ which is maximum in modulus. Fig. 5.b shows an example of application of relation (28) when $m_s = 7$. Note that substituting relation (28) in (21) one obtains the maximum and minimum current vectors ${}^{\omega}\mathbf{I}_M$ and ${}^{\omega}\mathbf{I}_{\underline{M}}$ corresponding to the maximum and minimum torques $\tau_M(\omega_m)$ and $\tau_{\underline{M}}(\omega_m)$. From the previous considerations it is clear that the maximum torque control is obtained choosing ${}^{\omega}\mathbf{I}_d = {}^{\omega}\mathbf{I}_M$ when $\tau_d \ge \tau_M(\omega_m)$ and ${}^{\omega}\mathbf{I}_d = {}^{\omega}\mathbf{I}_{\underline{M}}$ when $\tau_d \le \tau_{\underline{M}}(\omega_m)$. In Fig. 6 the two curves $\tau_M(\omega_m)$ and $\tau_{\underline{M}}(\omega_m)$ define in the torque plane the withe region that represents the zone not allowed because τ_d cannot exceed the maximum and minimum torque. Due to the symmetric structure of the considered electric motor, it can be easily shown that $\tau_M(\omega_m) = -\tau_{\underline{M}}(-\omega_m)$ (see Fig. 6).

4.3 Convex combination torque control

In Fig. 6 the curves τ_N, $\tau_{\underline{N}}$, τ_M and $\tau_{\underline{M}}$ define a red zone in the (τ_m, ω_m) plane that represents the region where the two previous control laws can not be used. In this case the optimal control law which satisfies the voltage constraint (6) and minimizes the current dissipation is quite complex and difficult to be found. In this case we propose to use the following suboptimal control law obtained as convex combination of the previous defined current vectors. When $\omega_m < \omega_L$ and $\tau_N < \tau_d < \tau_M$ or $\tau_{\underline{M}} < \tau_d < \tau_{\underline{N}}$, the torque τ_d is obtained as follows using the current vectors ${}^{\omega}\mathbf{I}_N$, ${}^{\omega}\mathbf{I}_M$, ${}^{\omega}\mathbf{I}_{\underline{N}}$ and ${}^{\omega}\mathbf{I}_{\underline{M}}$:

$$ {}^{\omega}\mathbf{I}_d = \begin{cases} {}^{\omega}\mathbf{I}_{cc} = {}^{\omega}\mathbf{I}_N + \alpha\,({}^{\omega}\mathbf{I}_M - {}^{\omega}\mathbf{I}_N) & \text{if } \tau_N < \tau_d < \tau_M \\ {}^{\omega}\mathbf{I}_{\underline{cc}} = {}^{\omega}\mathbf{I}_{\underline{N}} + \underline{\alpha}\,({}^{\omega}\mathbf{I}_{\underline{M}} - {}^{\omega}\mathbf{I}_{\underline{N}}) & \text{if } \tau_{\underline{M}} < \tau_d < \tau_{\underline{N}} \end{cases} $$

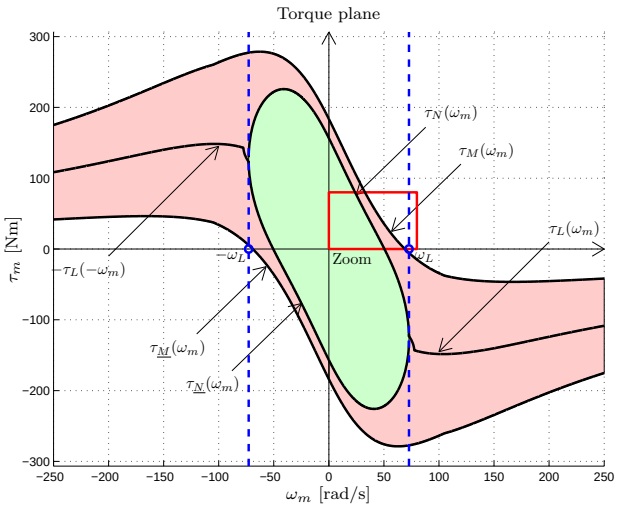

Figure 6. Maximum torque τ_M, minimum torque $\tau_{\underline{M}}$, maximum torque satisfying minimum dissipation τ_N, minimum torque satisfying minimum dissipation $\tau_{\underline{N}}$ and limit torque τ_L as a functions of motor velocity.

where coefficients α and $\underline{\alpha}$ are defined as follows:

$$\alpha = \frac{\tau_d - \tau_N(\omega_m)}{\tau_M(\omega_m) - \tau_N(\omega_m)}, \qquad \underline{\alpha} = \frac{\tau_d - \tau_{\underline{N}}(\omega_m)}{\tau_{\underline{M}}(\omega_m) - \tau_{\underline{N}}(\omega_m)}.$$

When $\omega_m > \omega_L$ the curves τ_N and $\tau_{\underline{N}}$ are not exist than it is necessary to define the limit torque τ_L or in equivalent way the limit current vector ${}^{\omega}\mathbf{I}_L$. The components of ${}^{\omega}\mathbf{I}_L$ are obtained as:

$$\begin{aligned} &I_{dk} = 0, && I_{qk} = I_{qkN} && \text{if } R_{0k}^2 > X_{0k}^2 \\ &I_{dk} = X_{0k} - R_{0k}, && I_{qk} = Y_{0k} && \text{otherwise.} \end{aligned}$$

In this case the convex combination can be written as:

$${}^{\omega}\mathbf{I}_d = \begin{cases} {}^{\omega}\mathbf{I}_{ccL} = {}^{\omega}\mathbf{I}_L + \alpha_L\,({}^{\omega}\mathbf{I}_M - {}^{\omega}\mathbf{I}_L) & \text{if } \tau_L < \tau_d < \tau_M \\ {}^{\omega}\mathbf{I}_{\underline{ccL}} = {}^{\omega}\mathbf{I}_L + \underline{\alpha}_L\,({}^{\omega}\mathbf{I}_{\underline{M}} - {}^{\omega}\mathbf{I}_L) & \text{if } \tau_{\underline{M}} < \tau_d < \tau_L \end{cases}$$

where the coefficients α_L and $\underline{\alpha}_L$ are defined as follows:

$$\alpha_L = \frac{\tau_d - \tau_L(\omega_m)}{\tau_M(\omega_m) - \tau_L(\omega_m)}, \qquad \underline{\alpha}_L = \frac{\tau_d - \tau_L(\omega_m)}{\tau_{\underline{M}}(\omega_m) - \tau_L(\omega_m)}.$$

A graphical representation of this control law for $m_s = 5$ is shown in Fig. 7 and in Fig. 8. The green and black circles represent the current circles $\mathcal{C}_k$ obtained using the minimum dissipation control and the maximum control. Note that there are only two black circles because the maximum voltage constraint $V_{\overline{M}}$ is applied only to the component $V_{\overline{M}k}$ in subspace $\Sigma_{\omega k}$ that satisfied eq. (28). The red lines $\overline{I}_{cck}$ and $\overline{I}_{ccLk}$, represent the convex combination on the complex planes when $\omega_m < \omega_L$ and $\omega_m \geq \omega_L$. The magenta and the blue lines show how the convex combination start and end points $\overline{I}_{Nk}$,$\overline{I}_{Lk}$ and $\overline{I}_{Mk}$ move in the complex planes $\Sigma_{\omega k}$ when the velocity ω_m increases.

4.4 Global torque control

Putting together the previous three controllers one obtains the following global control law for choosing vector ${}^{\omega}\mathbf{I}_d$.

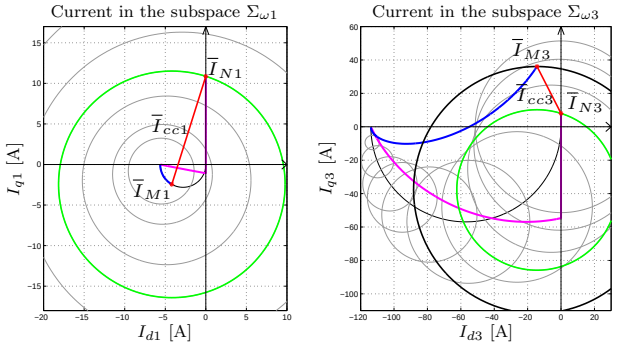

Figure 7. Graphical representation of the convex combination control for $m_s = 5$ and $\omega_m < \omega_L$.

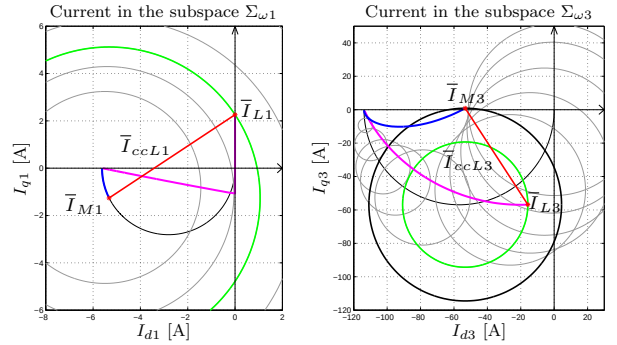

Figure 8. Graphical representation of the convex combination control for $m_s = 5$ and $\omega_m \geq \omega_L$.

If $\omega_m < \omega_L$ then:

$${}^{\omega}\mathbf{I}_d = \begin{cases} {}^{\omega}\mathbf{I}_M & \text{if } \tau_d \geq \tau_M(\omega_m) \\ {}^{\omega}\mathbf{I}_{cc} & \text{if } \tau_N(\omega_m) < \tau_d < \tau_M(\omega_m) \\ {}^{\omega}\mathbf{I}_{md} & \text{if } \tau_{\underline{N}}(\omega_m) \leq \tau_d \leq \tau_N(\omega_m) \\ {}^{\omega}\mathbf{I}_{\underline{cc}} & \text{if } \tau_{\underline{M}}(\omega_m) < \tau_d < \tau_{\underline{N}}(\omega_m) \\ {}^{\omega}\mathbf{I}_{\underline{M}} & \text{if } \tau_d \leq \tau_{\underline{M}}(\omega_m) \end{cases} \tag{29}$$

else:

$${}^{\omega}\mathbf{I}_d = \begin{cases} {}^{\omega}\mathbf{I}_M & \text{if } \tau_d \geq \tau_M(\omega_m) \\ {}^{\omega}\mathbf{I}_{ccL} & \text{if } \tau_L(\omega_m) < \tau_d < \tau_M(\omega_m) \\ {}^{\omega}\mathbf{I}_{\underline{ccL}} & \text{if } \tau_{\underline{M}}(\omega_m) < \tau_d < \tau_L(\omega_m) \\ {}^{\omega}\mathbf{I}_{\underline{M}} & \text{if } \tau_d \leq \tau_{\underline{M}}(\omega_m) \end{cases}$$

This control law, used together with relation (12), provides the desired torque τ_d satisfying the voltage constraint (6) and minimizing, when possible, the current dissipation.

5. SIMULATION

The multi-phase electric motor shown in Fig. 2 has been implemented in Simulink together with the control law (12) and (29). The simulation results described in this section have been obtained using the following electrical and mechanical parameters: $m_s = 7$, $p = 1$, $R_s = 2\,\Omega$, $L_s = 0.03$ H, $M_{s0} = 0.025$ H, $\varphi_r = 0.02$ W, $J_m = 1.6$ kg m^2, $b_m = 0.4$ Nms/rad, $V_{max} = 100$V, $a_1 = 0.2$, $a_3 = 0.45$, $a_5 = 0.35$. The external torque τ_e is zero until $t = 10$ s then $\tau_e = 45$ Nm (see the magenta dashed line in Fig. 9). The time behaviors of motor velocity ω_m, motor torque τ_m, desired torque τ_d, external torque τ_e and maximum torques τ_M and τ_N are shown in Fig. 9. The letters A, B, C, D and E refer to the critical points for the control: A when $\tau_d = \tau_N$, B and D when $\tau_d = \tau_M$, C when

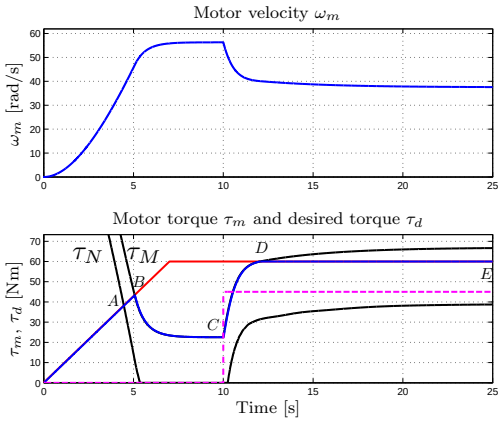

Figure 9. Time behaviors of motor velocity ω_m, motor torque τ_m (blue), desired torque τ_d (red), external torque τ_e (magenta) and maximum torques τ_M and τ_N (black).

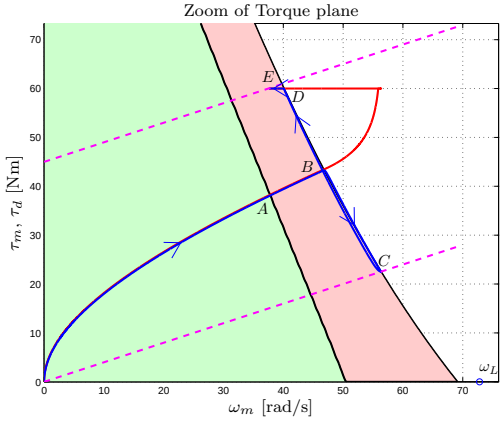

Figure 10. Motor torque τ_m (blue), desidered torque τ_d (red) and maximum torques τ_M and τ_N (black) as a function of motor velocity ω_m.

the external torque τ_e is applied and E the finaly stady state condition. Note that for $\tau_d \leq \tau_M$, i.e. from point 0 to point B and from point D to point E, the control law (12) and (29) guarantees $\tau_m = \tau_d$. The graphical representation of the torque curves $\tau_M(\omega_m)$ and $\tau_N(\omega_m)$ in Fig. 10 has been obtained eliminating the time variable from the two pictures of Fig. 9. The current vectors $\overline{I}_{sk}$ in the two-dimensional subspaces $\Sigma_{\omega k}$ and the time behaviors of modulus $V_{\overline{M}k}$ are shown in Fig. 11. The desired torque τ_d is provided only by the quadrature components I_{qk} of the current vectors $\overline{I}_{sk}$ until $\tau_d = \tau_N$ in point A. Note that from A to B, where the convex combination control ${}^{\omega}\mathbf{I}_{cc}$ is used, the current and voltage vectors $\overline{I}_{sk}$ remain within the maximum limit circles $\mathcal{C}_k$. From point B to point D the maximum torque control ${}^{\omega}\mathbf{I}_M$ is used, the desired torque τ_d is generated only by the current component I_{q5M} and the maximum voltage constraint $V_{\overline{M}}$ is applied only to the component $V_{\overline{M}5}$ in subspace $\Sigma_{\omega 5}$. From D to E the desired torque τ_d is provided by the convex combination control.

6. CONCLUSION

In this paper the torque control of multi-phase synchronous machines is analyzed. A new control law which satisfies the input voltage constraint and minimizes the current power dissipation has been proposed. The optimal-

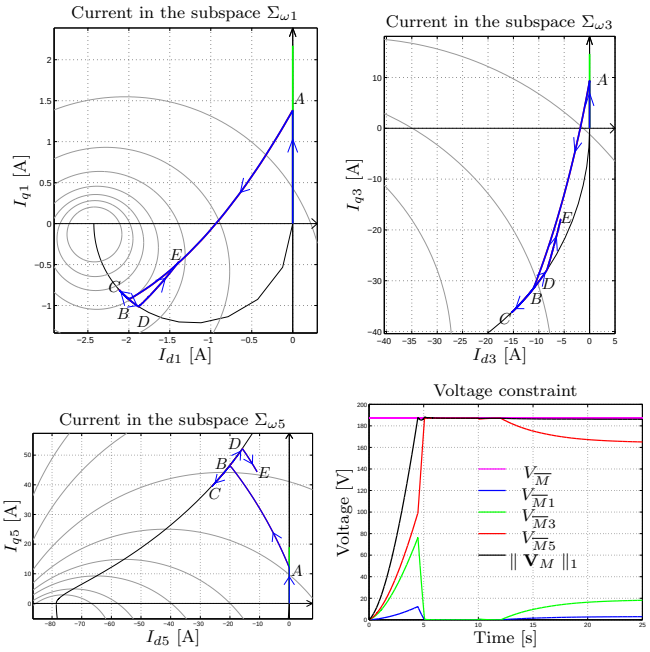

Figure 11. Current vectors $\overline{I}_{sk}$ and voltages vectors $\overline{V}_{sk}$ in the two-dimensional subspaces $\Sigma_{\omega k}$.

ity of this control law is guaranteed when the minimum dissipation control or the maximum control are applied. Simulation results obtained in Simulink validated the effectiveness of the presented control law.

REFERENCES

P. Vas. *Vector Control of AC Machines.* Clarendon press, Oxford, 1990.

W. Leonhard. *Control of Electrical Drives*, 3rd Edition 2001, Springer-Verlag Berlin Heidelberg NewYork, ISBN 3-540-41820-2.

X. Kestelyn, E. Semail, JP. Hautier. *Vectorial Multimachine Modeling for a Five-Phase Machine.* In Proc. Int. Conf. Electrical Machines (ICEM), Bruges, Belgium, 2002, CD-ROM, Paper 394.

X. Kestelyn, E. Semail, JP. Hautier. *Right Harmonic Spectrum for the Back-Electromotive Force of a n-phase Synchronous Motor* Industry Application Conference, 2004, 39th IAS Annual Meeting, ISBN: 0-7803-8486-5.

R. Zanasi. *Power Oriented Modelling of Dynamical System for Simulation.* IMACS Symp. on Modelling and Control of Technological System, Lille, France, May 1991.

R. Zanasi. *Dynamics of a n-links Manipulator by Using Power-Oriented Graph.* SYROCO '94, Capri, Italy, 1994.

R. Zanasi, F. Grossi. *The POG technique for modelling multi-phase permanent magnet synchronous motors.* 6th EUROSIM Congress on Modelling and Simulation, Ljubljana, 9-13 September 2007.

R. Zanasi, F. Grossi. *Optimal Rotor Flux Shape for Multi-phase Permanent Magnet Synchronous Motors.* International Power Electronics and Motion Control Conference, September 1-3 2008, Poznan, Poland.

R. Zanasi, F. Grossi. *Vectorial Control of Multi-phase Synchronous Motors using POG Approach.* IECON 2009, 35th Annual Conference of the IEEE Industrial Electronics Society, November 3-5, 2009 Porto, Portugal.